World Journal of Advanced Research and Reviews
eISSN: 2581-9615 CODEN (USA): WJARAI
Cross Ref DOI: 10.30574/wjarr
Journal homepage: https://wjarr.com/

(RESEARCH ARTICLE)

Check for updates

Feature extraction and fusion using deep convolutional neural networks for Covid-19 detection using CT and X-RAY images

Abdulhamit SUBASI [1, 2], Tugce KELES [3, *], Fatih OZYURT [4], Sengul DOGAN [3] and Turker TUNCER [3]

[1] *Institute of Biomedicine, Faculty of Medicine, University of Turku, 20520, Turku, Finland.*
[2] *Department of Computer Science, College of Engineering, Effat University, Jeddah, 21478, Saudi Arabia.*
[3] *Department of Digital Forensics Engineering, College of Technology, Firat University, Elazig/ Turkey.*
[4] *Department of Software Engineering, College of Engineering, Firat University, Elazig/ Turkey.*

World Journal of Advanced Research and Reviews, 2023, 19(01), 914–933

Publication history: Received on 02 June 2023; revised on 14 July 2023; accepted on 16 July 2023

Article DOI: https://doi.org/10.30574/wjarr.2023.19.1.1391

Abstract

COVID-19 represents a novel variant of the coronavirus disease, having rapidly disseminated across the globe. In recent studies pertaining to computer vision, image processing, and classification techniques, numerous methodologies have been introduced employing chest X-ray images and computerized tomography (CT) images. This investigation introduces novel fused deep features founded on CT and X-ray image classification, with the aim of detecting COVID-19 disease. The proposed approach encompasses three key phases: deep feature generation, iterative feature selection, and classification. During the feature generation phase, well-known pre-trained deep convolutional neural networks, namely DenseNet201, MobileNetV2, ResNet18, ResNet50, ResNet101, VGG16, and VGG19, were leveraged. Each network model generated 1000 features, which were subsequently fused, culminating in the acquisition of a final feature vector comprising 7000 dimensions. In order to distill the most pertinent information, the ReliefF and iterative maximum relevance minimum redundancy (RFImRMR) feature selection techniques were employed in the generation of the ultimate feature vector. To evaluate the performance of the proposed method, publicly available datasets of CT images and X-ray images were employed. Notably, the suggested deep learning approach attained accuracy rates of 99.33% and 93.10% for COVID-19 detection using CT and X-ray images, respectively. These achieved results serve as compelling evidence substantiating the efficacy of the proposed fused deep features and RFImRMR-based COVID-19 detection.

Keywords: Fused deep features; COVID-19 detection; RFImRMR feature selection; Computer vision; Image Classification; Deep Learn

1. Introduction

In December 2019, an emergent deadly virus surfaced, rapidly disseminating on a global scale and instigating a worldwide pandemic (1, 2). This affliction, denoted COVID-19 by the esteemed World Health Organization (WHO) (3), manifests as an acute respiratory illness. Person-to-person transmission serves as the primary means of contagion. According to the latest WHO report, the United States has encountered the highest number of cases, with 2,949,455 instances and 165,311 fatalities. Europe ranks second with 2,191,614 cases and 183,313 deaths. The WHO report, encompassing 6,287,771 cases and 379,941 deaths, garners considerable attention worldwide (4). Nations have enacted diverse policies and measures in an attempt to mitigate the epidemic, including the quarantine of infected individuals, implementation of curfews, temporary suspension of in-person education, mandatory mask usage, enforcement of social distancing, and the closure of public venues (5-7). These measures vary due to dissimilar

* Corresponding author Tugce KELES

protective policies across nations. Nevertheless, their overarching objective remains consistent: to minimize transmission risks, enable early disease detection, isolate infected patients, and diminish the mortality rate (8, 9).

Typical symptoms associated with COVID-19 encompass cough, fever, and fatigue. In severe cases, patients may experience dyspnea, chest pain, loss of mobility, and speech impairment. In conjunction with clinical manifestations, the detection of COVID-19 relies on the utilization of CT scans, X-ray images, and pathogenic tests (10-13). Pathogenic tests, predicated on the reverse transcription-polymerase chain reaction (RT-PCR) methodology, entail an examination of viral RNA. However, in instances where COVID-19 testing is unavailable, CT scans and X-ray images can serve as diagnostic aids (4, 14). Such imaging modalities may unveil abnormalities prior to RT-PCR test results turning positive. Moreover, high-resolution chest CT scans and X-ray assessments can detect subtle details, including ground-glass opacities, thereby rendering them highly sensitive for COVID-19 identification. Consequently, experts gain enhanced insight into the spatial distribution of pulmonary lesions via CT scans and X-ray images (15).

1.1. Motivations

The primary objective of this study is to introduce a highly accurate approach for COVID-19 detection utilizing CT and X-ray images. In this research, we aim to evaluate the effectiveness of deep learning methods in the context of feature engineering. Our proposed method involves the utilization of deep fused features and RFImRMR for CT and X-ray image classification, with the intention of harnessing the most informative and impactful features to achieve superior performance. The feature generation challenge is addressed by employing widely recognized pre-trained convolutional neural networks (CNNs). Furthermore, we present a novel iterative and hybrid (two-layered) feature selection approach, aiming to select distinctive features effectively and determine the optimal size of the final feature vector.

As evidenced by the existing literature, numerous works have been introduced to accurately detect COVID-19, predominantly utilizing deep learning models. However, these prior models suffer from certain limitations, namely:

- They solely employ either CT or X-ray image datasets.
- Generally, a single deep learning model is applied to the image dataset, without leveraging the advantages of alternative deep networks.
- The feature generation phases in previous models are deficient, often lacking a robust feature selector.

To address these limitations, we have developed novel fused deep features and an RFImRMR feature selector-based automatic COVID-19 detection model. Our proposed approach leverages seven transfer learning models for extracting deep features, while RFImRMR efficiently selects the most relevant features from the pool of 7,000 generated features. To demonstrate the universal classification capability of our model, both CT and X-ray image datasets have been utilized.

1.2. Proposed Approach

This study presents a straightforward yet highly effective approach for COVID-19 detection based on CT and X-ray images. The approach encompasses three key phases: deep feature generation using seven widely adopted pre-trained CNN models, meaningful feature selection employing the proposed RFImRMR feature selector, and classification utilizing a deep learning-based classifier. It is well established in the literature that deep learning techniques exhibit superior performance in image classification tasks (16, 17).

To gauge the effectiveness of the most commonly employed pre-trained CNN models, we introduced a fused deep feature generation network/method. This approach leverages these models as feature generators, extracting 1000 features from each transfer learning model and concatenating them to yield a final feature vector size of 7000. To address the issue of feature redundancy and reduce the dimensionality of the feature vector, we propose a two-layered feature selector combining ReliefF and iterative mRMR. This selector effectively decreases the size of the final feature vector while retaining the most informative features. Subsequently, RFImRMR is applied to the resulting feature vector of size 7000. The selected feature vector is then utilized as input for the deep classifier.

By employing this comprehensive approach encompassing feature generation, selection, and classification, we aim to achieve accurate COVID-19 detection using CT and X-ray images.

1.3. Novelties and Contribution

The novel contributions of the presented fused deep features and RFImRMR model can be summarized as follows:

The model's universality in image classification is demonstrated by testing it on both X-ray and CT images. This comprehensive evaluation allows for a broader understanding of the model's capabilities in detecting COVID-19.

The study highlights the efficacy of seven commonly used deep feature extraction models by employing them for feature generation. These models, widely recognized in the computer vision domain, are combined in a hybrid feature extraction method. Additionally, the classification performance of these networks is thoroughly analyzed within this research.

A novel feature selection approach is introduced, combining two widely adopted feature selectors. ReliefF, known for its ability to identify redundant features, is used to eliminate such redundancies based on negative weights. Iterative mRMR is then applied to automatically select the best feature vector. This innovative feature selection function, named RFImRMR, addresses the challenge of automatically determining the most informative features.

The main contributions of this study can be summarized as follows:

The proposed hybrid and iterative feature selector, RFImRMR, tackles the problem of automatically determining the optimal number of features and considers the variable performance of different feature selectors. By leveraging ReliefF to identify redundant features and using iterative mRMR to select top features from the non-redundant set, this approach provides an effective solution.

A novel model is introduced that leverages deep features for medical image classification. The primary objective of this model is to exploit the strengths of seven transfer learning models collectively. The RFImRMR feature selection method is employed to choose the most distinctive and informative features. The presented fused deep feature and RFImRMR-based model is tested on both CT and X-ray image datasets, demonstrating high accuracies for both. However, it is important to note that the success of this model in different scenarios may vary, and further evaluation is needed. Furthermore, the model alleviates the challenge of selecting the most suitable pre-trained deep network by incorporating seven deep models.

In summary, this research contributes novel insights in feature selection and deep feature-based medical image classification, showcasing the effectiveness of the proposed fused deep features and RFImRMR model in detecting COVID-19 from CT and X-ray images.

2. Literature Review

Medical professionals widely employ CT scans and X-ray images to monitor disease progression and discriminate COVID-19 from other viral infections. The expeditious evaluation they provide serves as an additional rationale for their utilization. Extensive research has explored the impact of CT scans and X-ray imaging on COVID-19, leading to the development of automated recognition systems tailored for this purpose (18). These automated recognition systems streamline specialists' work and mitigate the risks of oversight. Table 1 catalogs select studies focused on COVID-19 diagnosis employing computed tomography (CT) and X-ray imaging techniques.

Wang et al. (31) presented a sophisticated model harnessing Inception transfer learning to diagnose COVID-19 from CT images. Their system utilized a dataset comprising 1,119 CT images from 259 patients, yielding an impressive accuracy rate of 89.5%. Zhao et al. (32) compiled a dataset of CT images with the aim of investigating the impact of such images on COVID-19 diagnosis. Transfer learning was applied to the dataset, leading to a favorable evaluation of 275 data samples. The resulting accuracy rate reached 84.7%. Another contribution by Wang et al. (12) proposed a deep learning-based approach for COVID-19 diagnosis. The study involved a total of 630 CT images, divided into 499 training data and 131 test data. An accuracy rate of 90.8% was attained. The authors also calculated the execution time required for COVID-19 diagnosis. While the average time taken by a specialist doctor to diagnose COVID-19 on CT images was 300 seconds, their proposed method achieved a diagnosis time of merely 1.93 seconds.

Ardakani et al. (33) devised an automatic detection method utilizing deep learning techniques for COVID-19 diagnosis. The study incorporated 1,020 CT images from 108 COVID-19 patients, as well as CT images from 86 non-COVID-19 patients. The achieved accuracy rate amounted to an impressive 99.51%. Song et al. (34) introduced a deep learning-based system, named Deep Pneumonia, for diagnosing COVID-19 disease. The system leveraged CT images from 88 COVID-19 patients, 101 patients with bacterial pneumonia, and 86 healthy individuals. The evaluation metrics for the system included an Area Under the Curve (AUC) of 95%, an accuracy of 86.0%, a recall of 96.0%, a precision of 79.0%, and an F1-score of 87%.

Table 1 The review of related works

Study	Method	Classifier	Dataset	Type of Images	Split ratio	The results (%)
Ghassemi et al. (19)	Cyclic generative adversarial net	Softmax	189 samples	CT images	70:15:15	Acc: 99.20 Pre: 98.92 Rec: 98.92 F1: 99.10 AUC: 99.95
Khozeimeh et al. (20)	Convolutional neural networks, Autoencoder	Convolutional neural networks	520 samples	CT images	10 fold cross validation	Acc: 96.05 Rec: 98.00 Spe: 93.14 F1: 96.50 AUC: 95.55
Alizadehsani et al. (21)	Generative adversarial networks, Semi-supervised learning,	Convolutional neural networks	10.000 samples	CT images	80:20	Acc: 99.60 Sen: 99.39 Spe: 99.80
Chaudhary and Pachori (22)	Fourier-Bessel series expansion-based decomposition	Softmax	1. 785 samples 2. 2481 samples	CT images	5 fold cross validation	Acc: 1. 100.0 2. 97.60
Nayak et al. (23)	Convolutional neural networks	Softmax	406 samples	Chest X-ray images	70:30	Acc: 98.33
Ardakani et al. (24)	Statistical analysis	Ensemble	612 samples	CT images	80:20	Acc: 91.94 Spe: 90.32 Sen:93.54
Waheed et al. (25)	Convolutional neural networks, generative adversarial networks	Softmax	1124 samples	Chest X-ray images	932 training 192 testing	Acc: 95.00 Sen: 90.00 Spe: 97.00
Narin et al. (26)	Convolutional neural networks	Softmax	1. 3141 samples	Chest X-ray images	5 fold cross validation	Acc: 1. 96.10

			2. 1834 samples 3. 3113 samples			2. 99.50 3. 99.70
Pathak et al. (27)	Deep convolutional neural networks	Softmax	852 samples	Chest CT images	10 fold cross validation	Acc: 93.01
Abbas et al. (28)	Convolutional neural networks	Softmax	196 samples	Chest X-ray images	70:30	Acc: 93.10
Mangal et al. (29)	Deep neural network	Deep neural network	6014 samples	Chest X-ray images	80:20	Acc: 90.50 Sen: 100.0
Pereira et al. (7)	Local binary pattern, Elongated quinary patterns, Local directional number, Locally encoded transform feature histogram, Binarized statistical image features, Local phase quantization, Oriented basic image features, Convolutional neural networks	Predictive Cluster Trees and generates a single Decision Tree	1144 samples	Chest X-ray images	70:30	F1: 88.89
Apostolopoulos and Mpesiana (30)	Convolutional neural networks	Convolutional neural networks	1427 samples	Chest X-ray images	10 fold cross validation	Acc: 96.78 Sen: 98.66 Spe: 96.46

Zheng et al. (35) developed a novel model based on deep neural networks specifically designed for COVID-19 diagnosis. The proposed system achieved an accuracy rate of 90.1%. Butt et al. (36) contributed a deep learning-based COVID-19 detection system utilizing CT images. Their dataset consisted of 618 individuals, including 219 COVID-19 cases, 224 pneumonia cases, and 175 healthy individuals. The accuracy rates calculated reached 86.7%. Lastly, Al-karawi et al. (37) introduced a novel method for COVID-19 disease detection named FFT-Gabor, which relies on Fast Fourier Transform and Gabor Filter techniques. Their study employed CT images, achieving high accuracy (95.37%), sensitivity (95.99%), and specificity (94.76%) values. Loey et al. (38) introduced a study focused on detecting COVID-19 disease using CT images, employing transfer learning models such as ResNet50, VGGNet16, AlexNet, GoogleNet, and VGGNet19. The ResNet50 architecture emerged as the most effective model, achieving an accuracy ratio of 82.91%. Ozturk et al. (39) proposed an automated detection method for COVID-19 disease utilizing X-ray images. The performance of their deep learning method was evaluated, resulting in accuracy rates of 98.08% and 87.02% respectively.

Minaee et al. (40) devised a deep transfer learning model named Deep-COVID for COVID-19 disease detection. The classification of COVID-19 disease was conducted based on X-ray images. Notably, the study reported a sensitivity of 98.00% and a specificity of 90.7% for ResNet18.

Rajaraman et al. (41) developed a study centered on using convolutional neural networks with chest X-rays for COVID-19 disease detection. The study encompassed three classes: bacterial, COVID-19, and normal. The weighted averaging (pruned) approach achieved an accuracy rate of 99.01%.

Khan et al. (6) proposed a deep neural network model named CoroNet for COVID-19 detection. The study employed chest X-ray images for testing the model's efficacy. In the case of the proposed method involving four classes (normal, COVID-19, viral pneumonia, bacterial pneumonia), an accuracy rate of 89.6% was obtained. Furthermore, an accuracy rate of 95% was achieved for the three-class scenario (COVID-19, pneumonia, normal).

3. Materials and method

3.1. The used datasets

This research utilizes two publicly available datasets comprising CT and X-ray images. The CT image dataset consists of two classes: normal and COVID-19. The dataset contains a total of 746 CT images, with 349 images classified as COVID-19 and 397 images classified as normal. These images were sourced from GitHub data repositories, and no ethical approval was required for their use (32). To provide a visual representation, Figure 1 displays a selection of sample images from this dataset.

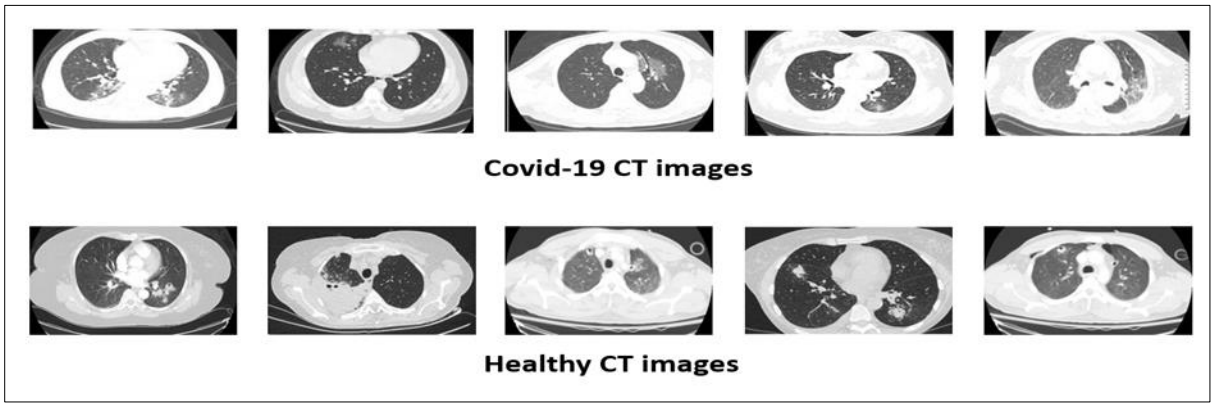

Figure 1 Sample images of the CT image dataset used for COVID-19 detection. This dataset contains COVID-19 and healthy

The X-ray image dataset encompasses three classes: Normal, COVID-19, and Pneumonia. It comprises a total of 1125 X-ray images, including 500 normal, 125 COVID-19, and 500 pneumonia images (39). Figure 2 showcases sample X-ray images from this dataset, providing a glimpse into its content.

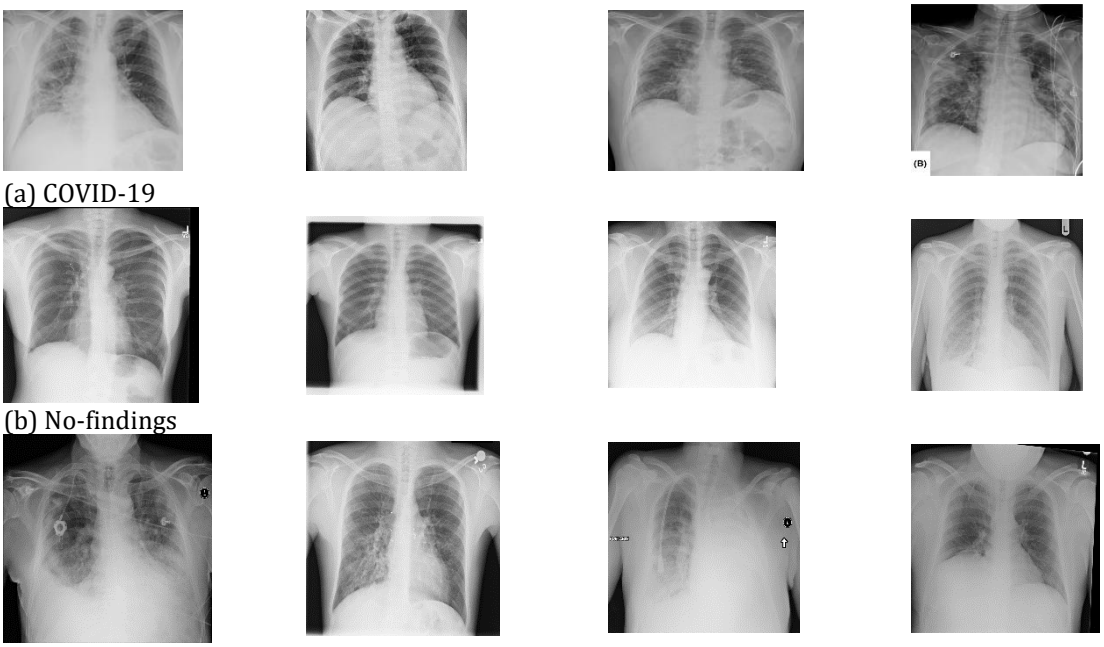

(a) COVID-19

(b) No-findings

(c) Pneumonia

Figure 2 Sample images of the X-ray image dataset used for COVID-19 detection. This dataset contains COVID-19, No-findings, and Pneumonia

3.2. Preliminaries

In this section, we provide a brief overview of the seven pre-trained CNN models utilized in our study, with more detailed information available in references (42-44). These models have gained significant popularity in the field of computer vision, making them suitable choices for feature extraction. Each model generates 1000 features through the application of its respective pre-trained architecture. The following are the key details of the selected networks:

- **DenseNet 201:** The DenseNet architecture (45, 46) achieved the top-1 classification error in the ImageNet ILSVRC-2012 dataset competition. It employs approximately 20 million parameters, demonstrating remarkable success with half the parameters of other architectures. DenseNet layers establish explicit connections with all preceding layers within a pooling zone, facilitating feature reuse and promoting information flow throughout the network.
- **MobileNetV2:** Developed by the Google team (47), MobileNetV2 builds upon the concepts of MobileNetV1, incorporating deeply separable convolutions as an effective building block. Two notable additions in V2 are linear bottlenecks between layers and shortcut links between bottlenecks. This lightweight architecture, featuring deeply separable convolutional layers, offers flexibility in balancing performance and efficiency by adjusting global hyperparameters according to specific problem criteria.
- **ResNet18, ResNet50, and ResNet101:** ResNet (48), introduced in 2015, revolutionized deep CNN training by addressing the vanishing gradient problem through the inclusion of identity links between layers. ResNet architectures, consisting of convolutional, pooling, activation, and fully connected layers, stack these components to create deep residual networks. ResNet18 comprises two-layer blocks, while ResNet50 and ResNet101 employ three-layer blocks. The FLOP (floating point operations) count for ResNet18 is approximately 1.8 billion, while ResNet50 and ResNet101 architectures involve 3.8 billion and 7.6 billion FLOPs, respectively.
- **VGG16 and VGG19:** Simonyan and Zisserman introduced the VGG network architecture in 2014 (49). VGGnet emerged as the winner in the ILSVRC 2014 competition for image localization and classification tasks. The hallmark of VGG networks lies in their simplicity, utilizing stacked layers of 3x3 convolutional filters to increase depth. The numerical designations "16" and "19" in VGG–16 and VGG–19 signify the respective numbers of layers in each architecture.

3.3. The Proposed Framework

This research introduces a novel approach for accurate COVID-19 detection by leveraging fused deep features and the RFImRMR feature selector. The presented model consists of three key steps: fused deep feature generation, informative

feature selection using RFImRMR, and classification employing a deep classifier. To provide a comprehensive understanding of the proposed framework, we outline the steps below.

Step 0: Load the CT or X-ray image.

Step 1: Apply the DenseNet201, MobileNetV2, ResNet18, ResNet50, ResNet101, VGG16, and VGG19 deep networks to the CT or X-ray images. These seven networks have been extensively trained on the ImageNet dataset, which comprises millions of images across 1000 categories. By leveraging the knowledge gained from training on ImageNet, these pre-trained networks can extract optimal features from the medical images. In our approach, we employ the pre-trained networks in a feed-forward manner to generate deep features. By utilizing these deep features, abnormalities can be easily detected, as the networks capture both low-level and high-level features, thereby enhancing accuracy.

The proposed fused deep feature generator is a parametric method that can incorporate multiple pre-trained deep networks. In this study, we select the widely used seven CNNs, including DenseNet201, MobileNetV2, ResNet18, ResNet50, ResNet101, VGG16, and VGG19. DenseNet201 is recognized for its high accuracy, while MobileNetV2 stands out as a renowned CNN model. ResNets and VGGNets have gained widespread popularity in various image classification applications. By utilizing these seven networks with their default parameters, we harness the effectiveness of these networks collectively within our model.

Step 2: Extract 1000 features from each network.

Step 3: Concatenate these features to obtain the final feature vector (X) with a size of 7000.

Step 4: Apply ReliefF (50) to the feature vectors and eliminate features with negative weights. Negative weighted features are considered redundant and are therefore removed.

Step 5: Employ iterative mRMR to select features with positive weights.

Step 6: Select the feature vector with the minimum loss value, representing the best set of features.

Step 7: Feed these selected features into the deep classifier to obtain classification results.

For a visual representation of the proposed framework, refer to Figure 3, which depicts the graphical illustration of the fused deep features and RFImRMR-based approach.

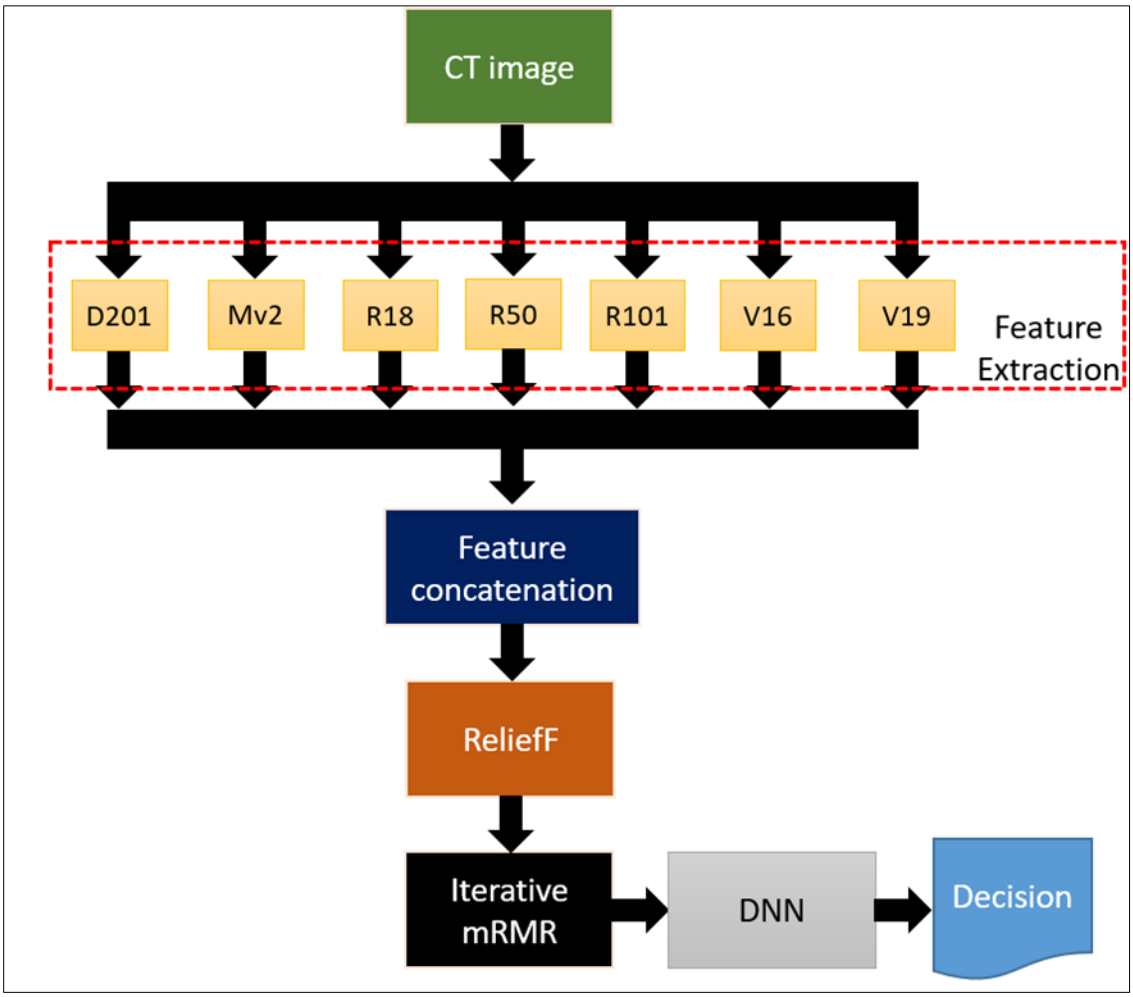

Figure 3 The schematic expression of the proposed fused deep features and RFImRMR based COVID-19 detection method.

Figure 3 illustrates the graphical representation of our approach, where D201, Mv2, R18, R50, R101, V16, and V19 correspond to DenseNet201, MobileNetv2, ResNet18, ResNet50, ResNet101, VGG16, and VGG19 CNNs, respectively. The ReliefF and iterative mRMR boxes signify the RFImRMR feature selector proposed in this study. The features selected by RFImRMR serve as the input to the classifier. The depicted steps in Figure 3 provide a visual overview of our method. In the subsequent subsections, we delve into the primary phases of our model, elucidating their details.

3.3.1. Fused Deep Feature Generation

This phase holds significant importance within the presented framework. The seven CNNs employed in this phase, namely DenseNet201, MobileNetv2, ResNet18, ResNet50, ResNet101, VGGNet16, and VGGNet19, were trained using the extensive ImageNet dataset (51). These networks serve as feature extractors, yielding 1000 features from each of them. The fusion of these extracted features results in a total of 7000 features. Our primary objective revolves around proposing a novel feature engineering model, wherein pre-trained networks play a pivotal role. Leveraging the transfer learning approach eliminates the need for weight assignment. By utilizing these pre-trained networks alongside the feature extraction layer (preceding the softmax layer), deep feature extractors can be employed. These deep feature extractors possess several key attributes: they generate features at various levels, ranging from low to moderate and high. Through the utilization of a hybrid and iterative feature selector, essential features can be selected. Furthermore, this study underscores the elimination of the necessity to train specific CT or X-ray image datasets for accurate COVID-19 detection. By leveraging the optimal weights acquired through training on the ImageNet dataset, precise biomedical image classification models can be proposed. We have validated the validity of this proposition specifically for COVID-19 in our research. To enhance comprehension of our fused deep feature generation model, we define the feature generation function of these networks as follows:

$D201(.), Mv2(.), R18(.), R50(.), R101(.), V16(.)$ and $V19(.)$ for DenseNet201, MobileNetv2, ResNet18, ResNet50, ResNet101, VGGNet16 and VGGNet19 respectively. Steps of our feature generator are;

1: Extract 1000 features by using seven used deep feature generation function.

$$ft^1 = D201(I^k) \quad (1)$$
$$ft^2 = Mv2(I^k) \quad (2)$$
$$ft^3 = R18(I^k) \quad (3)$$
$$ft^4 = R50(I^k) \quad (4)$$
$$ft^5 = R101(I^k) \quad (5)$$
$$ft^6 = V16(I^k) \quad (6)$$
$$ft^7 = V19(I^k) \quad (7)$$

where ft^k k[th] feature of the deep fused features used with a length of 1000 and I^k represents the k[th] CT or X-ray image on the used dataset.

2: Concatenate these feature vectors to obtain final features.

$$X\big((k-1)*1000+j\big) = ft^k(j), k = \{1,2,\dots,7\} \quad (8)$$

As stated from Eq. 8, the final feature vector (X) has 7000 features.

3.3.2. Feature Selection

In this research, we introduce a novel hybrid feature selector that effectively identifies the most distinctive features from the pool of 7000 extracted features. This selector combines the ReliefF and iterative mRMR feature selection methods, which are widely recognized and proven to be effective in computer vision. However, it is worth noting that neither of these methods autonomously determines the optimal number of informative features.

A relevant study by Huang et al. (52) presented a multilabel feature selection approach that leveraged Relief and mRMR to enhance the classification performance of multilabel data. They employed Relief and mRMR jointly to improve the success rate of feature selection. In our research, we adopt ReliefF and iterative mRMR as our feature selection methods. ReliefF, an advanced variant of the Relief feature selector, assigns weights to each individual feature. It effectively identifies redundant features by assigning them negative weights, which can subsequently be eliminated using the iterative mRMR. As a result, ReliefF is employed in the initial phase of our proposed RFImRMR method. In the subsequent step, the iterative mRMR method is applied to the features selected by ReliefF. The iterative mRMR method tackles the challenge of automatically selecting the optimal number of features. The primary objective of the presented RFImRMR method is to automatically determine the most suitable number of features per classifier, harnessing the effectiveness of both ReliefF and mRMR selectors.

The mathematical formulation of the ReliefF and mRMR algorithms is as follows: ReliefF utilizes the Manhattan distance metric to calculate weights, generating both negative and positive weights. Negative weights are assigned to redundant features within the ReliefF method. While the traditional Relief-based feature selection method employs the Euclidean distance metric, ReliefF utilizes the Manhattan distance to generate weights. The mathematical representation of the weight generation process based on ReliefF is provided in Equations 9-12.

$$WR(ft_i) = WR(ft_i) - \frac{\sum_{j=1}^{k} dist(A,T,N)}{n*k} + \frac{\sum_{C\neq class(R)}\left[\frac{Pr(C)}{1-Pr(R)} * \sum_{l=1}^{k} dist(A,T,M)\right]}{n*k} \quad (9)$$

$$dist(A,L_1,L_2) = \begin{cases} 0, L_1 = L_2 \\ 1, L_1 \neq L_2 \end{cases} \quad (10)$$

$$dist(A,L_1,L_2) = \frac{|L_1 - L_2|}{A_{max} - A_{min}} \quad (11)$$

The mRMR feature selection algorithm is the minimum redundancy maximum relevance (mRMR) algorithm, which is selected by simultaneously optimizing the minimum redundancy and maximum relevance conditions. Either the redundancy between features or the relevance between features and corresponding classes is measured by mutual

information (MI) in the mRMR algorithm. In order to calculate the similarity among features and feature tags, MI should be calculated as the formula below.

$$I(X,Y) = \sum_{y\in Y}\sum_{x\in X}(x,y)\ \log\left(\frac{p(x,y)}{p_1(x)\,p_2(y)}\right) \tag{12}$$

The schematic explanation of the presented RFImRMR is denoted in Figure 4.

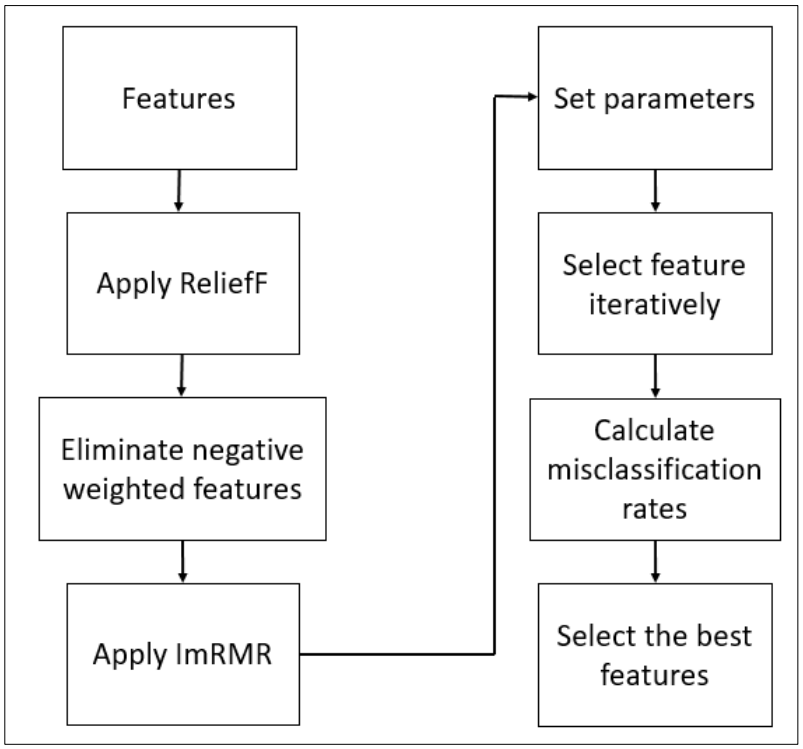

Figure 4 The graphical explanation of the RFImRMR selector

Steps of the RFImRMR are;

1: Apply ReliefF on the features extracted (X) and calculate 7000 weights.

$$weight = ReliefF(X, target) \tag{13}$$

2: Select positive weighted features.

$$f^R(i) = X(j), if\ weight(j) > 0\ and\ i = i + 1 \tag{14}$$

where f^R represents selected features by ReliefF.

3: Employ mRMR to generate sorted indices.

$$idx = mRMR(f^R) \tag{15}$$

where idx defines sorted indices.

4: Create a loop to 100 from 1000 for iterative feature selection using idx.

$$fs^{h-99}(j) = fs^{h-99}\big(idx(j)\big), h = \{100,101,\dots,1000\}, j = \{1,2,\dots,h\} \tag{16}$$

5: Calculate loss values by using the nearest neighbor (NN) classifier. NN is one of the fastest classifiers for the small/medium datasets. The loss value calculator is selected as DNN to decrease the computational complexity of the proposed RFImRMR feature selector.

$$loss(h-99) = kNN(fs^{h-99}, target, 10) \quad (17)$$

where *loss* represents loss value, and to calculate loss value 10-fold CV is used.

6: Calculate the index of the minimum error value.

$$[mini, index] = \min(loss) \quad (18)$$

$$index = index + 99 \quad (19)$$

where *mini* and *index* are minimum value and index of the minimum values.

7: Select the last features by using *index* value calculated.

$$opt(j) = fs^{index-99}\big(idx(j)\big), j = \{1,2,\dots,index\} \quad (20)$$

The RFImRMR feature selector, as presented in this research, effectively identifies and selects a subset of features that exhibit superior discriminatory capabilities from the initial set of 7000 features. Specifically, on the CT image dataset, the RFImRMR selector identifies and retains 841 features out of the total 7000 features. Similarly, on the X-ray image dataset, the RFImRMR selector intelligently chooses 578 features from the initial pool of 7000 features. This selective feature extraction process ensures that the resulting feature set maintains high relevance and discriminative power, contributing to the accurate detection and classification of COVID-19 cases.

3.3.3. Classification

For classification purposes, we employed a Deep Neural Network (DNN)(53) classifier in this study. To ensure robust validation and testing, a 10-fold cross-validation (CV) strategy was adopted. The DNN utilized is a backpropagation network, and we employed the scaled conjugate backpropagation (tainscg) algorithm to determine the optimal weights of the network.

In the backpropagation algorithm, we employed a scaled conjugate gradient (SCG) optimization technique, setting the learning rate to 0.7, momentum to 0.3, and batch size to 100. To explore the remaining DNN hyperparameters, we conducted an exhaustive manual search procedure, calculating the classification accuracy using 10-fold cross-validation for each parameter configuration.

Through this meticulous process, we identified the best-performing DNN architecture, consisting of three hidden layers with 200, 100, and 50 nodes, respectively. This architecture demonstrated superior performance in terms of classification accuracy (refer to Fig. 5).

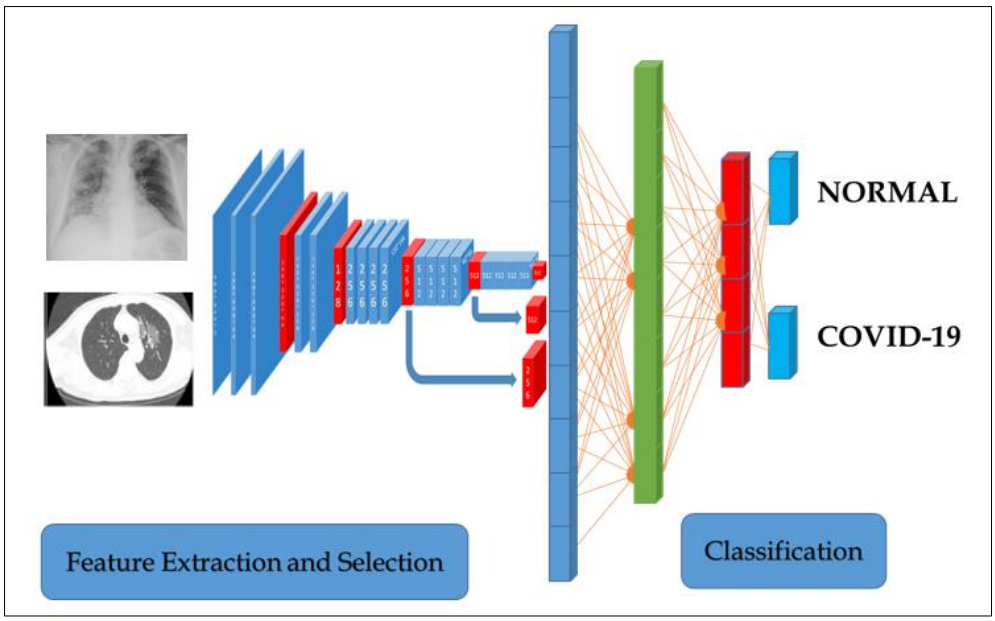

Figure 5 The presentation of Deep Feature Extraction and Deep Learning Model

4. Results

The proposed model was implemented in the MATLAB programming environment (version 2019a). We leveraged the pre-trained networks defined in the feature extraction phase to conduct our experiments. Specifically, we extracted 1000 features from the fully connected layers of these networks. To combine these features, a basic MATLAB code was developed for feature concatenation.

For the RFImRMR feature selection method, we coded a dedicated function in MATLAB to facilitate its implementation. To assess the model's performance, we employed the widely adopted 10-fold cross-validation (CV) technique to compute various measurements. The DNN classifier was utilized to obtain the classification results.

To evaluate the model's effectiveness, we computed several performance metrics using the confusion matrices obtained. These metrics include accuracy, balanced accuracy, precision, recall, F1-score, specificity, geometric mean, false-negative rates, and false-positive rates. The mathematical definitions of these performance metrics can be found in Table 2.

Table 2 Performance metrics used for evaluation of the proposed model. To calculate these performance metrics number of true positives (TP), true negatives (TN), false positives (FP), and false negatives (FN) should be used

Name	Equation	Equation number
Accuracy	$\frac{tp + tn}{tp + tn + fp + fn}$	(21)
Balanced accuracy/ unweighted average recall	$\frac{1}{C}\left(\frac{tp}{tp + fn} + \frac{tn}{tn + fp}\right)$	(22)
Precision	$\frac{tp}{tp + fp}$	(23)
Recall/ Sensitivity	$\frac{tp}{tp + fn}$	(24)
F1	$2\frac{Precision * Recall}{Presicion + Recall}$	(25)
Specificity	$\frac{tn}{tn + fp}$	(26)
Geometric mean	$\sqrt{Recall * Specificity}$	(27)

The comprehensive evaluation of the proposed fused deep features and RFImRMR-based COVID-19 detection approach was carried out using nine predefined performance metrics. The resulting confusion matrices for each dataset can be found in Tables 3 and 4.

Table 3 Confusion matrix of CT Dataset

Actual class	Predicted class		Recall
	COVID-19	Healthy	
COVID-19	347	2	99.42%
Healthy	3	394	99.24%
Precision	99.14%	99.49%	99.33%

Table 4 Confusion matrix of the X-ray Dataset

Actual class	**Predicted class**			**Recall**
	Normal	COVID-19	Pneumonia	
Normal	461	0	39	92.20%
COVID-19	0	122	3	97.60%
Pneumonia	38	3	459	91.80%
Precision	92.38%	97.60%	91.61%	93.10%

These tables present the precision, recall, and accuracy values achieved by the proposed per classifier. Specifically, the X-ray image dataset attained a classification accuracy of 93.10%, while the CT image dataset achieved an accuracy of 99.33%. The corresponding measurements for each dataset can be found in Table 5.

Table 5 The Performance Metrics (%) of the proposed Framework using DNN

Measurement	**X-ray**	**CT**
Accuracy	93.10±0.3	99.33±0.16
Balanced accuracy/ unweighted average recall	93.87±0.1	99.33±0.17
Precision	93.87±0.08	99.14±0.7
Recall/ Sensitivity	93.87±0.1	99.42±0.19
F1	93.87±0.23	99.28±0.08
Specificity	92.20±0.76	99.24±0.01
Geometric mean	93.83±0.25	99.33±0.18

Table 5 showcases the remarkable performance of the proposed approach in achieving a classification accuracy of 99.33% for the CT image dataset. This dataset consists of two classes, namely COVID-19 and healthy. Conversely, the X-ray image dataset comprises three classes: Normal, COVID-19, and Pneumonia. Our deep fused method has achieved a commendable classification accuracy of 93.10% for this dataset.

Through experimental studies, it has been observed that utilizing 7000 features obtained from seven distinct CNN architectures, without incorporating feature engineering, yielded a success rate of 97.31% for the CT image dataset and 90.76% for the X-ray image dataset. To facilitate a comprehensive comparison of the proposed fused deep features and ImRMR-based COVID-19 detection model across the datasets, the results have been graphically depicted in Figure 6.

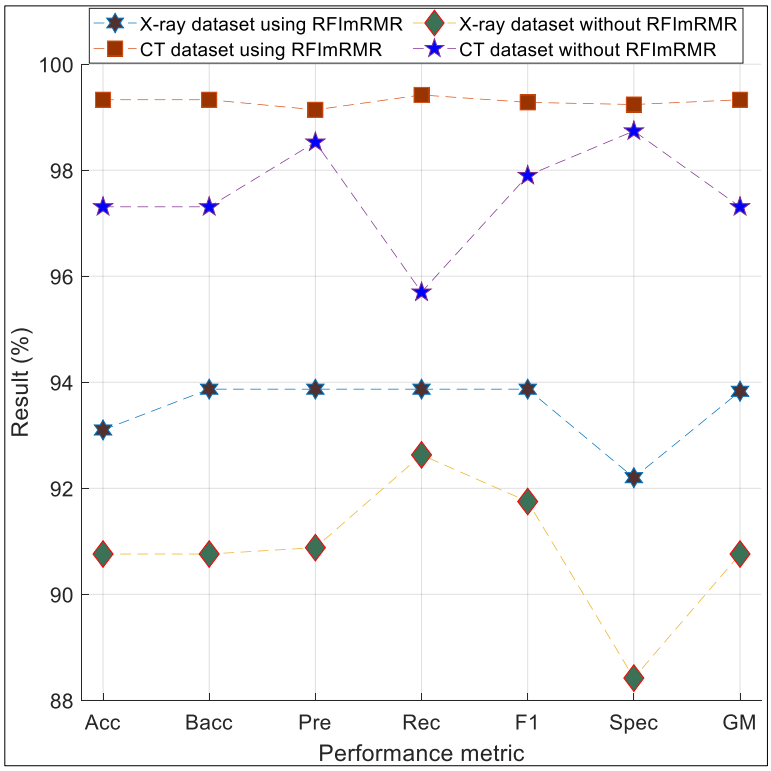

Figure 6 Results of our proposal. Acc, Bacc, Pre, Rec, F1, and GM express accuracy, balanced accuracy, precision, recall, F1-score, specificity, and geometric mean consecutively

5. Discussions

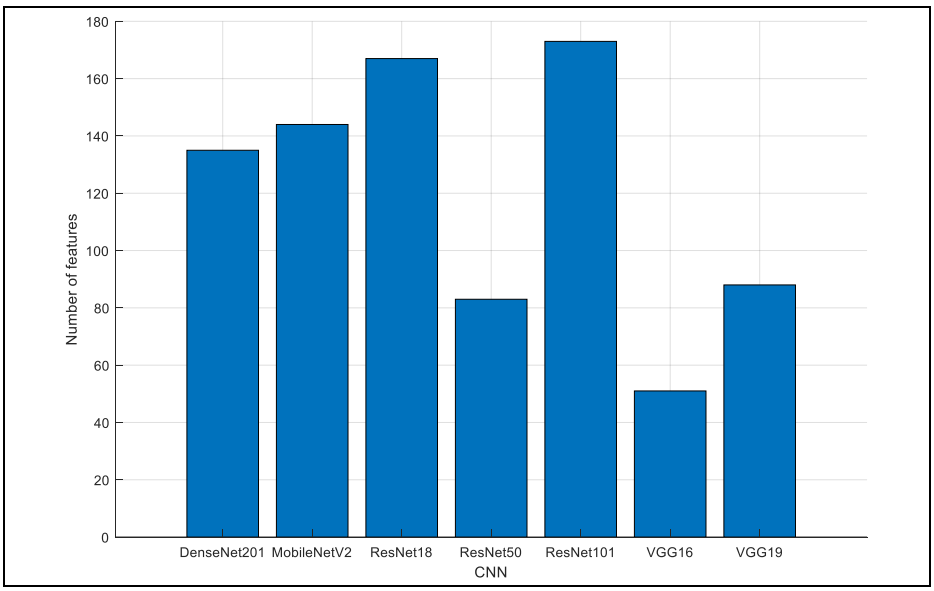

Figure 7 Distribution of features according to deep networks. The final feature vector consists of 135 features of DenseNet201, 144 features of MobileNetv2, 167 features of ResNet18, 83 features of ResNet50, 173 features of ResNet101, 51 features of the VGGNet16, and 88 features of VGGNet19. This distribution belongs to the CT image dataset.

This study presents a novel COVID-19 detection model that utilizes fused deep features and the RFImRMR feature selector. The primary goal of this COVID-19 detection model is to achieve exceptional classification performance by leveraging pre-trained deep networks and employing iterative and hybrid feature selectors. In the context of feature engineering, this research focuses on evaluating the efficacy of deep learning methods. Consequently, the proposed

RFImRMR aims to identify the most influential features. The RFImRMR methodology comprises two essential layers: ReliefF and iterative mRMR. The initial set of 7000 extracted features is passed through ReliefF, which selects 5351 features with positive weights. Subsequently, iterative mRMR assesses these selected features and identifies the 841 most informative features for the CT image dataset. In the case of the X-ray image dataset, the RFImRMR selector chooses 578 features. As mentioned in the feature generation section, seven distinct deep networks are employed, thus resulting in the final feature vector encompassing features from these networks. To provide a comprehensive understanding of the impact of each deep network, the number of features contained within each network is depicted in Figure 7.

Table 6 Previous studies using XRAY images

Study	Used dataset	Method	Accuracy (%)
(39)	125 COVID-19 500 Healthy 500 Pneumonia	DarkCovidNet	87.02
(4)	25 COVID-19 25 Healthy	COVIDX-Net	90.0
(54)	224 COVID-19 504 Healthy 700 Pneumonia	VGG-19	93.48
(55)	25 COVID-19 25 Healthy	ResNet50þ SVM	95.38
(56)	100 COVID-19 200 Healthy 322 Pneumonia	Convolutional neural network	95.74
(57)	135 COVID-19, 150 Healthy 150 Pneumonia	F-transform, MKLBP and SVM	97.01
(58)	150 COVID-19 150 Healthy	ShuffleNet+NCA+Relief	99.98
Proposed Method	500 Normal, 125 COVID-19, and 500 Pneumonia	Fused deep feature& RFImRMR	93.10

Table 7 Previous studies using CT images

Study	Used dataset	Method	Accuracy (%)
(38)	UCSD-AI4H	CGAN	82.9
(32)	UCSD-AI4H	TL+CSSL	89.1
(34)	777 COVID-19 708 Healthy (Private Dataset)	DRE-Net	86.0
(36)	219 COVID-19 175 Healthy 224 Pneumonia (Private Dataset)	ResNet Location Attention	86.7
(31)	325 COVID-19 740 Healthy (Private Dataset)	M-Inception	89.5
(35)	313 COVID-19 229 Healthy (Private Dataset)	DeCoVNet	90.8
(37)	275 COVID-19 195 Healthy (Private Dataset)	FFT-Gabor	95.4

(59)	UCSD-AI4H	Deep Learning+NCA	88.0
(60)	UCSD-AI4H	FDEPFGN	95.54
Proposed Method	UCSD-AI4H	Fused deep feature& RFImRMR	99.33

Upon reviewing the existing literature, it becomes evident that the recommended method showcased the highest performance rate compared to previous studies. Table 6 provides an overview of academic research utilizing CT images for COVID-19 detection. By comparing the performance metrics reported in these studies, it is apparent that our proposed approach outperforms the alternatives, emphasizing its superiority in terms of accuracy and efficacy.

While the literature lacks a substantial number of studies focusing on the diagnosis of COVID-19 using CT images, Table 7 provides insights into the existing research endeavors. Notably, our proposed study achieved an impressive success rate of 99.33% (as indicated in Table 7). It is worth highlighting that our study surpasses the performance of the studies listed in Tables 6 and 7, exhibiting a remarkable success rate that is 15% higher than those using the same dataset. This significant margin underscores the efficacy and triumph of our proposed approach.

The advantages of the chest CT and X-ray image classification method, based on our novel deep feature extraction and RFImRMR feature selection techniques, can be summarized as follows:

Advantages:

- Introduction of a pioneering pre-trained deep feature extraction method.
- Proposal of an innovative RFImRMR feature selection method.
- Attainment of impressive accuracies of 93.10% and 99.33% for the X-ray and CT image datasets, respectively.
- Cognitive nature of the method, eliminating the need to set millions of parameters as in deep learning networks.
- Outperformance of seven comparative studies employing chest CT and X-ray images (See Tables 6 and 7).
- Demonstration of the universal classification capability of our proposal, utilizing both CT and X-ray image datasets.

However, it is important to acknowledge certain limitations of our study, which include the following:

Limitations:

- The potential for utilizing a larger dataset to enhance the robustness of the tests.
- Exploration of more lightweight models for efficient classification of these images.

6. Conclusion

Amidst the global turmoil caused by the pandemic in 2020, numerous studies have emerged focusing on the detection of COVID-19 utilizing CT and X-ray images. In line with this context, our study presents a novel method for diagnosing COVID-19 from CT and X-ray images, employing a deep feature and RFImRMR-based cognitive approach. To assess the effectiveness of our proposed method, various performance metrics including Accuracy, Balanced Accuracy/Unweighted Average Recall, Precision, Recall/Sensitivity, F1 score, Specificity, Geometric Mean, False-positive rate, and False-negative rate were computed for both image datasets. Remarkably, the proposed method outperformed all other approaches in both datasets. It is worth noting that the Deep Neural Network (DNN) exhibited the highest classifier performance among the methods evaluated.

Looking ahead, we envision the introduction of CNN-based architectures specifically designed for mobile programming, facilitating the detection of COVID-19. Furthermore, research and development efforts will be directed towards providing support for medical professionals in detecting COVID-19 from chest CT and X-ray images. Additionally, a concerted effort will be made to collect a more extensive collection of chest CT and X-ray images, enabling the detection of various lung diseases related to COVID-19.

By pursuing these future endeavors, we aim to make significant advancements in the field of COVID-19 detection, further empowering healthcare professionals in combating the pandemic.

Compliance with ethical standards

Acknowledgements

We thank the researchers who collect and openly share datasets in the literature.

Disclosure of conflict of interest

The authors declare that there is no conflict to interest related to this paper.

Funding

There is no funding source for this article.

References

[1] Pathak Y, Shukla PK, Tiwari A, Stalin S, Singh S. Deep transfer learning based classification model for COVID-19 disease. Irbm. 2022;43(2):87-92.

[2] Rothan HA, Byrareddy SN. The epidemiology and pathogenesis of coronavirus disease (COVID-19) outbreak. Journal of autoimmunity. 2020;109:102433.

[3] Cao X. COVID-19: immunopathology and its implications for therapy. Nature reviews immunology. 2020;20(5):269-70.

[4] Hemdan EE-D, Shouman MA, Karar ME. Covidx-net: A framework of deep learning classifiers to diagnose covid-19 in x-ray images. arXiv preprint arXiv:200311055. 2020.

[5] Shi F, Wang J, Shi J, Wu Z, Wang Q, Tang Z, et al. Review of artificial intelligence techniques in imaging data acquisition, segmentation, and diagnosis for COVID-19. IEEE reviews in biomedical engineering. 2020;14:4-15.

[6] Khan AI, Shah JL, Bhat MM. CoroNet: A deep neural network for detection and diagnosis of COVID-19 from chest x-ray images. Computer methods and programs in biomedicine. 2020;196:105581.

[7] Pereira RM, Bertolini D, Teixeira LO, Silla Jr CN, Costa YM. COVID-19 identification in chest X-ray images on flat and hierarchical classification scenarios. Computer methods and programs in biomedicine. 2020;194:105532.

[8] Ayoobi N, Sharifrazi D, Alizadehsani R, Shoeibi A, Gorriz JM, Moosaei H, et al. Time series forecasting of new cases and new deaths rate for COVID-19 using deep learning methods. Results in physics. 2021;27:104495.

[9] Shoeibi A, Khodatars M, Alizadehsani R, Ghassemi N, Jafari M, Moridian P, et al. Automated detection and forecasting of covid-19 using deep learning techniques: A review. arXiv preprint arXiv:200710785. 2020.

[10] Dai H, Zhang X, Xia J, Zhang T, Shang Y, Huang R, et al. High-resolution chest CT features and clinical characteristics of patients infected with COVID-19 in Jiangsu, China. International Journal of Infectious Diseases. 2020;95:106-12.

[11] Attivissimo F, Cavone G, Lanzolla AML, Spadavecchia M. A technique to improve the image quality in computer tomography. IEEE Transactions on Instrumentation and Measurement. 2010;59(5):1251-7.

[12] Wang X, Deng X, Fu Q, Zhou Q, Feng J, Ma H, et al. A weakly-supervised framework for COVID-19 classification and lesion localization from chest CT. IEEE transactions on medical imaging. 2020;39(8):2615-25.

[13] Barstugan M, Ozkaya U, Ozturk S. Coronavirus (covid-19) classification using ct images by machine learning methods. arXiv preprint arXiv:200309424. 2020.

[14] Alizadehsani R, Alizadeh Sani Z, Behjati M, Roshanzamir Z, Hussain S, Abedini N, et al. Risk factors prediction, clinical outcomes, and mortality in COVID-19 patients. Journal of medical virology. 2021;93(4):2307-20.

[15] Jahmunah V, Sudarshan VK, Oh SL, Gururajan R, Gururajan R, Zhou X, et al. Future IoT tools for COVID-19 contact tracing and prediction: a review of the state-of-the-science. International journal of imaging systems and technology. 2021;31(2):455-71.

[16] Özyurt F. Efficient deep feature selection for remote sensing image recognition with fused deep learning architectures. The Journal of Supercomputing. 2020;76(11):8413-31.

[17] Özyurt F. A fused CNN model for WBC detection with MRMR feature selection and extreme learning machine. Soft Computing. 2020;24(11):8163-72.

[18] Abbas A, Abdelsamea MM, Gaber MM. Classification of COVID-19 in chest X-ray images using DeTraC deep convolutional neural network. Applied Intelligence. 2021;51:854-64.

[19] Ghassemi N, Shoeibi A, Khodatars M, Heras J, Rahimi A, Zare A, et al. Automatic diagnosis of covid-19 from ct images using cyclegan and transfer learning. Applied Soft Computing. 2023:110511.

[20] Khozeimeh F, Sharifrazi D, Izadi NH, Joloudari JH, Shoeibi A, Alizadehsani R, et al. Combining a convolutional neural network with autoencoders to predict the survival chance of COVID-19 patients. Scientific Reports. 2021;11(1):15343.

[21] Alizadehsani R, Sharifrazi D, Izadi NH, Joloudari JH, Shoeibi A, Gorriz JM, et al. Uncertainty-aware semi-supervised method using large unlabelled and limited labeled COVID-19 data. arXiv preprint arXiv:210206388. 2021.

[22] Chaudhary PK, Pachori RB. FBSED based automatic diagnosis of COVID-19 using X-ray and CT images. Computers in Biology and Medicine. 2021;134:104454.

[23] Nayak SR, Nayak DR, Sinha U, Arora V, Pachori RB. Application of deep learning techniques for detection of COVID-19 cases using chest X-ray images: A comprehensive study. Biomedical Signal Processing and Control. 2021;64:102365.

[24] Ardakani AA, Acharya UR, Habibollahi S, Mohammadi A. COVIDiag: A clinical CAD system to diagnose COVID-19 pneumonia based on CT findings. European radiology. 2021;31(1):121-30.

[25] Waheed A, Goyal M, Gupta D, Khanna A, Al-Turjman F, Pinheiro PR. Covidgan: data augmentation using auxiliary classifier gan for improved covid-19 detection. Ieee Access. 2020;8:91916-23.

[26] Narin A, Kaya C, Pamuk Z. Automatic detection of coronavirus disease (covid-19) using x-ray images and deep convolutional neural networks. Pattern Analysis and Applications. 2021:1-14.

[27] Pathak Y, Shukla PK, Tiwari A, Stalin S, Singh S. Deep transfer learning based classification model for COVID-19 disease. Irbm. 2020.

[28] Abbas A, Abdelsamea MM, Gaber MM. Classification of COVID-19 in chest X-ray images using DeTraC deep convolutional neural network. Applied Intelligence. 2021;51(2):854-64.

[29] Mangal A, Kalia S, Rajgopal H, Rangarajan K, Namboodiri V, Banerjee S, et al. CovidAID: COVID-19 detection using chest X-ray. arXiv preprint arXiv:200409803. 2020.

[30] Apostolopoulos ID, Mpesiana TA. Covid-19: automatic detection from x-ray images utilizing transfer learning with convolutional neural networks. Physical and Engineering Sciences in Medicine. 2020;43(2):635-40.

[31] Wang S, Kang B, Ma J, Zeng X, Xiao M, Guo J, et al. A deep learning algorithm using CT images to screen for Corona Virus Disease (COVID-19). European radiology. 2021;31:6096-104.

[32] Yang X, He X, Zhao J, Zhang Y, Zhang S, Xie P. COVID-CT-dataset: a CT scan dataset about COVID-19. arXiv preprint arXiv:200313865. 2020.

[33] Ardakani AA, Kanafi AR, Acharya UR, Khadem N, Mohammadi A. Application of deep learning technique to manage COVID-19 in routine clinical practice using CT images: Results of 10 convolutional neural networks. Computers in biology and medicine. 2020;121:103795.

[34] Song Y, Zheng S, Li L, Zhang X, Zhang X, Huang Z, et al. Deep learning enables accurate diagnosis of novel coronavirus (COVID-19) with CT images. IEEE/ACM transactions on computational biology and bioinformatics. 2021;18(6):2775-80.

[35] Zheng C, Deng X, Fu Q, Zhou Q, Feng J, Ma H, et al. Deep learning-based detection for COVID-19 from chest CT using weak label. MedRxiv. 2020:2020.03. 12.20027185.

[36] Butt C, Gill J, Chun D, Babu BA. Deep learning system to screen coronavirus disease 2019 pneumonia. Appl Intell. 2020.

[37] Al-Karawi D, Al-Zaidi S, Polus N, Jassim S. Machine learning analysis of chest CT scan images as a complementary digital test of coronavirus (COVID-19) patients. MedRxiv. 2020:2020.04. 13.20063479.

[38] Loey M, Manogaran G, Khalifa NEM. A deep transfer learning model with classical data augmentation and CGAN to detect COVID-19 from chest CT radiography digital images. Neural Computing and Applications. 2020:1-13.

[39] Ozturk T, Talo M, Yildirim EA, Baloglu UB, Yildirim O, Acharya UR. Automated detection of COVID-19 cases using deep neural networks with X-ray images. Computers in biology and medicine. 2020;121:103792.

[40] Minaee S, Kafieh R, Sonka M, Yazdani S, Soufi GJ. Deep-COVID: Predicting COVID-19 from chest X-ray images using deep transfer learning. Medical image analysis. 2020;65:101794.

[41] Rajaraman S, Siegelman J, Alderson PO, Folio LS, Folio LR, Antani SK. Iteratively pruned deep learning ensembles for COVID-19 detection in chest X-rays. Ieee Access. 2020;8:115041-50.

[42] Ren S, Sun K, Tan C, Dong F. A two-stage deep learning method for robust shape reconstruction with electrical impedance tomography. IEEE Transactions on Instrumentation and Measurement. 2019;69(7):4887-97.

[43] Sutskever I, Martens J, Dahl G, Hinton G, editors. On the importance of initialization and momentum in deep learning. International conference on machine learning; 2013: PMLR.

[44] Erhan D, Courville A, Bengio Y, Vincent P, editors. Why does unsupervised pre-training help deep learning? Proceedings of the thirteenth international conference on artificial intelligence and statistics; 2010: JMLR Workshop and Conference Proceedings.

[45] Huang G, Liu Z, Van Der Maaten L, Weinberger KQ, editors. Densely connected convolutional networks. Proceedings of the IEEE conference on computer vision and pattern recognition; 2017.

[46] Pleiss G, Chen D, Huang G, Li T, Van Der Maaten L, Weinberger KQ. Memory-efficient implementation of densenets. arXiv preprint arXiv:170706990. 2017.

[47] Sandler M, Howard A, Zhu M, Zhmoginov A, Chen L-C, editors. Mobilenetv2: Inverted residuals and linear bottlenecks. Proceedings of the IEEE conference on computer vision and pattern recognition; 2018.

[48] He K, Zhang X, Ren S, Sun J, editors. Deep residual learning for image recognition. Proceedings of the IEEE conference on computer vision and pattern recognition; 2016.

[49] Simonyan K, Zisserman A. Very deep convolutional networks for large-scale image recognition. arXiv preprint arXiv:14091556. 2014.

[50] Robnik-Šikonja M, Kononenko I. Theoretical and empirical analysis of ReliefF and RReliefF. Machine learning. 2003;53:23-69.

[51] Deng J, Dong W, Socher R, Li L-J, Li K, Fei-Fei L, editors. Imagenet: A large-scale hierarchical image database. 2009 IEEE conference on computer vision and pattern recognition; 2009: Ieee.

[52] Huang M, Sun L, Xu J, Zhang S. Multilabel feature selection using relief and minimum redundancy maximum relevance based on neighborhood rough sets. IEEE Access. 2020;8:62011-31.

[53] Courbariaux M, Bengio Y, David J-P. Binaryconnect: Training deep neural networks with binary weights during propagations. Advances in neural information processing systems. 2015;28.

[54] Apostolopoulos ID, Mpesiana TA. Covid-19: automatic detection from x-ray images utilizing transfer learning with convolutional neural networks. Physical and engineering sciences in medicine. 2020;43:635-40.

[55] Sethy PK, Behera SK. Detection of coronavirus disease (covid-19) based on deep features. 2020.

[56] Zaki MA, Narejo S, Zai S, Zaki U, Altaf Z, u Din N. Detection of nCoV-19 from hybrid dataset of CXR images using deep convolutional neural network. International Journal of Advanced Computer Science and Applications. 2020;11(12).

[57] Tuncer T, Ozyurt F, Dogan S, Subasi A. A novel Covid-19 and pneumonia classification method based on F-transform. Chemometrics and intelligent laboratory systems. 2021;210:104256.

[58] Özyurt F. Automatic Detection of COVID-19 Disease by Using Transfer Learning of Light Weight Deep Learning Model. Traitement du Signal. 2021;38(1).

[59] Subasi A, Mitra A, Ozyurt F, Tuncer T. Automated COVID-19 detection from CT images using deep learning. Computer-Aided Design and Diagnosis Methods for Biomedical Applications: CRC Press; 2021. p. 153-76.

[60] Ozyurt F, Tuncer T, Subasi A. An automated COVID-19 detection based on fused dynamic exemplar pyramid feature extraction and hybrid feature selection using deep learning. Computers in biology and medicine. 2021;132:104356.